textiles

MDPI

Article

Structure versus Property Relationship of Hybrid Silk/Flax Composites

Heitor L. Ornaghi, Jr. [1,*], Roberta M. Neves [1], Lucas Dall Agnol [1], Eduardo Kerche [2] and Lidia K. Lazzari [1]

[1] Postgraduate Program in Processing Engineering and Technology (PGEPROTEC), Caxias do Sul University, R. Francisco Getúlio Vargas, Caxias do Sul 95070-560, Brazil; robertamneves@gmail.com (R.M.N.); lucasdall1989@hotmail.com (L.D.A.); lidia_lazzari@yahoo.com.br (L.K.L.)

[2] Postgraduate Program in Mining, Metallurgical and Materials Engineering, Federal University of Rio Grande do Sul (UFRGS), Porto Alegre 90040-060, Brazil; eduardo.fkerche@gmail.com

* Correspondence: hlornagj@ucs.br or ornaghijr.heitor@gmail.com

Abstract: The increasing demand for environmental and sustainable materials has motivated efforts to fabricate biocomposites as alternatives to conventional synthetic fiber composites. However, biocomposite materials have some drawbacks such as poor mechanical resistance, fiber/matrix incompatibility, low thermal resistance and high moisture absorption. Extensive research has been conducted to address these challenges, in terms of the sustainable production, serviceability, reliability and properties of these novel biocomposites. Silk fibers have excellent biocompatibility and biodegradability along with moderate mechanical properties, while flax fibers have a high specific strength and modulus. The combination of the silk fiber with moderate modulus and stiffness with flax fibers with high specific strength and modulus allows the modulation of the properties of silk using the intra- and inter-hybridization of both fibers. In this study, silk and flax fibers are combined in different arrangements, totaling eight different composites; the quasi-static mechanical properties and dynamic mechanical thermal analysis are discussed, focusing on the structure versus relationship properties, with the aim of corroborating the freely available data from literature. The main findings indicated that the synergic effect of the flax fiber and silk fiber leads to a tailormade composite with a low cost and high performance.

Keywords: natural fiber composites; hybrid composites; structure versus properties relationship

Citation: Ornaghi, H.L., Jr.; Neves, R.M.; Dall Agnol, L.; Kerche, E.; Lazzari, L.K. Structure versus Property Relationship of Hybrid Silk/Flax Composites. *Textiles* **2024**, *4*, 344–355. https://doi.org/10.3390/textiles4030020

Academic Editors: Rajesh Mishra, Tao Yang and Veerakumar Arumugam

Received: 27 June 2024
Revised: 25 July 2024
Accepted: 29 July 2024
Published: 1 August 2024

1. Introduction

Natural fiber composites are mainly implemented in low-level automobile industry applications such as door panels, instrument panels or seat shells [1]. In spite of the environmental appeal, biodegradability and lower cost compared with synthetic fibers, their use for high-level structural applications is still in the early stages of investigation [2]. To minimize the main drawbacks of natural fibers, it is common to "hybridize" the composite using a synthetic fiber such as carbon or glass, which reduces the final cost and weight of the final part [3,4]. Also, depending on the reinforcement configuration, the mechanical properties are not severely compromised [2]. The mechanical, chemical and thermal properties of natural fibers are affected but are not highly dependent on their chemical composition [5–8]. The reason is that, in spite of different individual characteristics of cellulose, hemicellulose and lignin, when these components are available in natural fibers, the overall behavior is quite similar for most of the fibers due to the availability of some physical/chemical interactions among some components [9]. To clarify, crystalline cellulose has higher mechanical properties than hemicellulose, which absorb more water. The higher water absorption capability decreases the mechanical properties of the entire fiber. If hemicellulose is removed from the fibers, lignin is affected because it serves as a bridge between the components. Hence, all components are interconnected to each other in a

higher or lower degree. Scheme 1 shows the schematic representation of the use of natural fibers in composite industry.

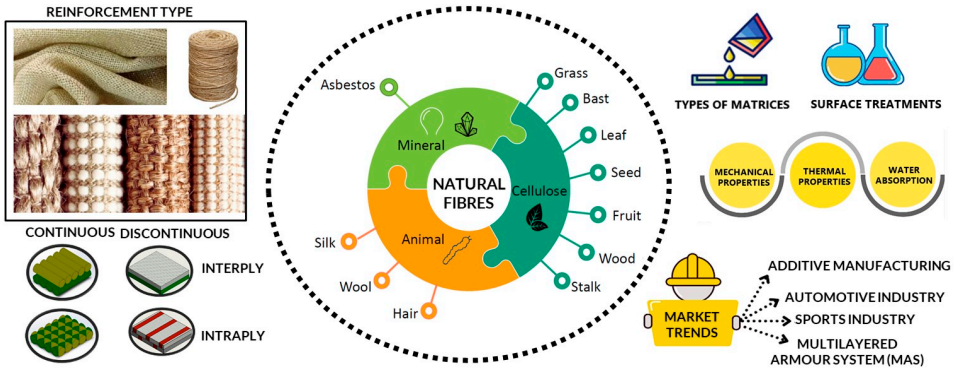

Scheme 1. Natural fiber and their applications in the composite industry. This figure was obtained under the Creative Commons Attribution 4.0 International License [10].

Flax fibers have superior mechanical properties than most natural fibers and have specific mechanical properties similar to glass fibers [11–13]. But due to the weak interfacial bonding with most polymeric matrices, low interlaminar strength and poor fracture toughness are expected [14–16]. Hence, the matrix/fiber interface and consequently the interlaminar strength and fracture toughness are expected to enhance by improving the matrix/fiber adhesion. This can be obtained by using modified nanomaterials, modifying the surface of the fibers, or hybridization with glass fiber, for example [17–20]. The main drawback in using nanoreinforcement is the high cost of the nanoparticles and the difficulty to disperse them, which complicates their use in an industrial context.

One of the most promising fibers to compensate for the low ductility and toughness of natural fiber composites commonly reinforced with sisal, jute or curaua is natural silk. There are four types of silk fibers produced around the world (Mulberry silk, Eri silk, Tasarsilk and Muga silk), with being Mulberry silk responsible for 90% of silk production [21,22]. One interesting characteristic is the ability of the silk fiber to absorb and dissipate energy simultaneously during deformation [23,24] and the possibility of using high volume fraction reinforcement (70 vol.%) to improve the mechanical behavior of epoxy resin. Yang et al. [25] studied silk/epoxy composites with a maximum reinforcement of 70 vol.% silk (varying from 30% to 70%). The tensile modulus (increases by 145%), breaking tensile energy (increases by 467%), flexural modulus (increases linearly up to 60%), ultimate flexural strength, breaking energy, interlaminar shear and impact strength (71 kJ m^{-2} for 60 vol.%) increase considerably compared to plain woven flax fiber. In addition to reinforcement, silk fiber has the potential to be used in biomedical applications for the reinforcement of biopolymers to enhance the stiffness of scaffoldings and bone implants [26], or in composite materials for task-specific applications [27]. However, the moderate strength, modulus and better interfacial bonding compared to the most common natural fibers such as sisal, jute or curaua [27–30] offsets their relatively high ductility and toughness.

Hybridization combines the characteristics of different types of fibers into a single matrix [31]. For example, Clarissa et al. [4] studied interlaminate glass/curaua hybrid composites at an overall fiber loading of 30 vol.% and a volume ratio of 1:1. Higher dissipation energy was found for the composites with four curaua grouped near the mid-plane. In a systematic review with papers selected from 2016 to 2020, Neves et al. [32] constated that, when properly combined, hybridization can combine the high performance of synthetic fiber with the ecological appeal of vegetal fiber. The authors described thermal, mechanical and dynamic mechanical thermal properties as well as their respective processing methods. The most employed manufacturing process was the hand lay-up, while the most common type of glass and vegetal fiber was woven fabric, being the most used interleaved composite. The authors also identified the main gaps in the literature on these types of composites,

which can be used as easily accessed guidelines, even for the most experienced researchers. One of the most used fibers for the improvement of impact strength in hybrid composites is basalt mineral fiber [33], although other natural fibers can be used for this purpose [34]. Basalt was also hybridized with silk fiber to assess the mechanical properties of epoxy composites and the best combination of properties (hardness, modulus and toughness) were found for silk/basalt at 25:25 wt.% [35]. Silk fiber is employed to improve fatigue resistance, light transmission and luminance distribution ability [36–38].

This study's objective is to re-use the data freely available in [39], aiming to promote an in-depth discussion regarding the structure vs. properties relationship and to complement the article published by Liu et al. [37]. In the study, neat epoxy resin and eight different composites were discussed in terms of density, tensile and flexural mechanical properties, dynamic mechanical thermal properties and interlaminar shear strength. New insights were offered from the results and the effects of flax fiber content and hybrid configuration were discussed.

2. Materials and Methods

2.1. Materials

The epoxy resin, silk and flax fabrics characteristics and suppliers are described in detail in [37]. Briefly, the silk and flax fabrics were obtained from Yi Bai Wang Industry Store. The epoxy/hardener (Araldite LY 1564/Araldur3486) were from Huntsman Corporation (Woodlands, TX, USA). Scheme 2 summarizes the materials used by the authors. The freely available data will be re-used, aiming to corroborate and complement the aforementioned article.

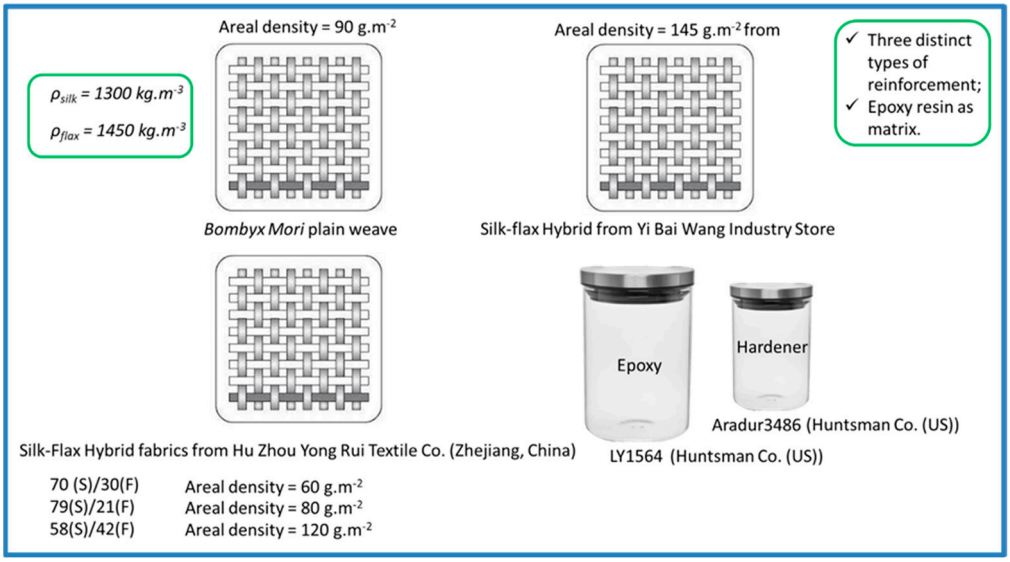

Scheme 2. Schematic representation of the reinforcements and matrices used in [37].

2.2. Composites

Besides neat epoxy resin, different composites were produced using a vacuum-assisted resin transfer molding process [37]. Briefly, the composites were fabricated in two stages: (i) vacuum-assisted resin transfer molding and (ii) hot pressing molding. Prior to resin infusion, the composites (dimensions of 200 mm × 100 mm) were dried in a vacuum oven at 70 °C for 12 h. A peel ply and distribution media were added to the top and bottom of the mold, while the reinforcement was put between them. The mold was covered with a vacuum bag and sealed with sealant. Prior to impregnation, the resin was degassed for 30 min. In the second stage, the composite was hot pressed at a pressure of 500 kPa for 8 h at 80 °C. The fabrication method and physical and mechanical tests are also presented in detail in [37]. Briefly, the tensile mechanical tests were performed on dog-bone specimens

(115 mm × 25 mm × 2 mm) using an Instron 8801 (Norwood, MA, USA) at a displacement rate of 2 mm·min^{-1}. The DMTA tests were performed in a DMA Q800 instrument under the cantilever mode from 25 °C to 170 °C at 3 °C·min^{-1} and at a frequency of 1 Hz. The composites and the respective volume fraction are presented on Table 1 and schematically represented in Scheme 3.

Table 1. Epoxy resin and composites studied in this work. The same nomenclature was used from the original study.

Composite	V_{total} (Fiber Volume Fraction) (%)	V_{silk} (Silk Fiber Volume Fraction) (%)	V_{flax} (Flax Fiber Volume Fraction) (%)
Silk reinforced/SB	50	50	0
Silk/flax hybrid fiber reinforced-FS1	48	20	28
Silk/flax hybrid fiber reinforced-FS2	51	15.3	35.7
Silk/flax hybrid fiber reinforced-FS3	47.5	10	37.5
Silk/flax hybrid fiber reinforced-HSH	52	29.7	22.3
Silk/flax hybrid fiber reinforced-SHS	51	38.2	12.8
Silk/flax hybrid fiber reinforced-SHI	51	35	16
Flax reinforced/FF	48	0	48
Pristine epoxy resin	0	0	0

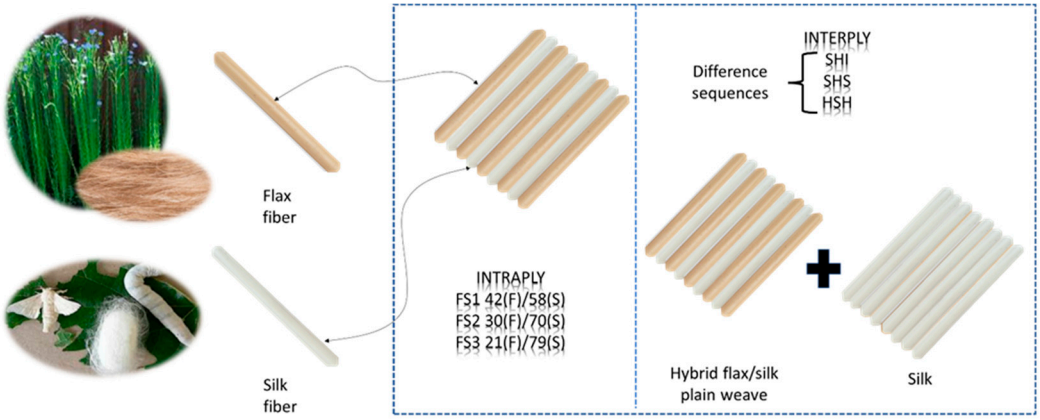

Scheme 3. Schematic representation of different configurations of the composites studied in this work.

FS1, FS2 and FS3 refer to 42:58, 30:70 and 21:79 silk/flax mix ratio, respectively. HSH refers to six silk fabrics as the core and five 30:70 silk/flax hybrid fabrics as skins. SHS refers to silk fabrics as skins and hybrid fabrics as the core. SHI refers to eight 30:70 silk/flax hybrid layers and seven silk fiber fabrics alternatively plied, keeping silk/flax hybrid layers as the outermost layers.

3. Results

Figure 1a–d represents the mechanical tests of the composites studied. Figure 1a shows the stress x strain curves for the neat resin, silk composite (SB) and the intraply composites (FS1, FS2 and FS3). The ductile behavior observed for the neat resin is considerably reduced when compared to SB, which also increases the elastic modulus. For the hybrid composites, as flax content increases in relation to silk fiber, a higher modulus is obtained with a smaller reduction in the strain. According to Figure 1b, the specific strength and specific modulus also increases for resin < SB < FS1 < FS2 < FS3. For FS2 and FS3, the values can be considered as similar. The breaking energy, shown in Figure 1c, shows the opposite effect of Figure 1b; the material becomes more fragile with the increase in the modulus. Figure 1d demonstrates a trend where, as the volume fraction of the fiber increases, the specific strength and modulus become higher, which is also expected with the exception of the 60% vol of flax fiber due to different fabric textile structures. Table 2 shows the mechanical properties compiled. It is noted that the Young's modulus is lower for the neat epoxy resin,

as expected. The composite reinforced only with silk fiber presented a value of 5.9 GPa, while the composite reinforced only with flax fiber (FF) presented a value of 11.8 GPa. The higher value of FF can be attributed to the higher tensile modulus of its own fibers [40]. As the overall volume fraction can be considered constant (~50 vol.%), the differences can be attributed to different configurations of the composites and the matrix/fiber interfacial characteristics. The stress transfer mechanism in polymer occurs through the amorphous polymeric chains, i.e., the more rigid the structural unit (monomer), the more energy is required to impose deformation into the polymeric chains, and the higher the modulus [41]. Since the external energy imposed is transferred to the polymeric chains, some portions of the chains reptate, aiming to dissipate the energy received as heat (the more rigid the structural unit, the more energy is required). If a reinforcement is incorporated into the "fragile" matrix, the stress imposed is transmitted through the interface for the fibers [42,43]. In this case, the interface quality and the fiber resistance play a major role in the final result of the measured property. Hence, there is an expected hindrance of the reptation movement of the amorphous polymeric chains because most of the energy imposed is received by the fibers though the interface. In this case, the amorphous polymeric chains of the polymeric matrix become a kind of "carrier of the energy" received and are no longer the main component responsible for the mechanical property [44–47].

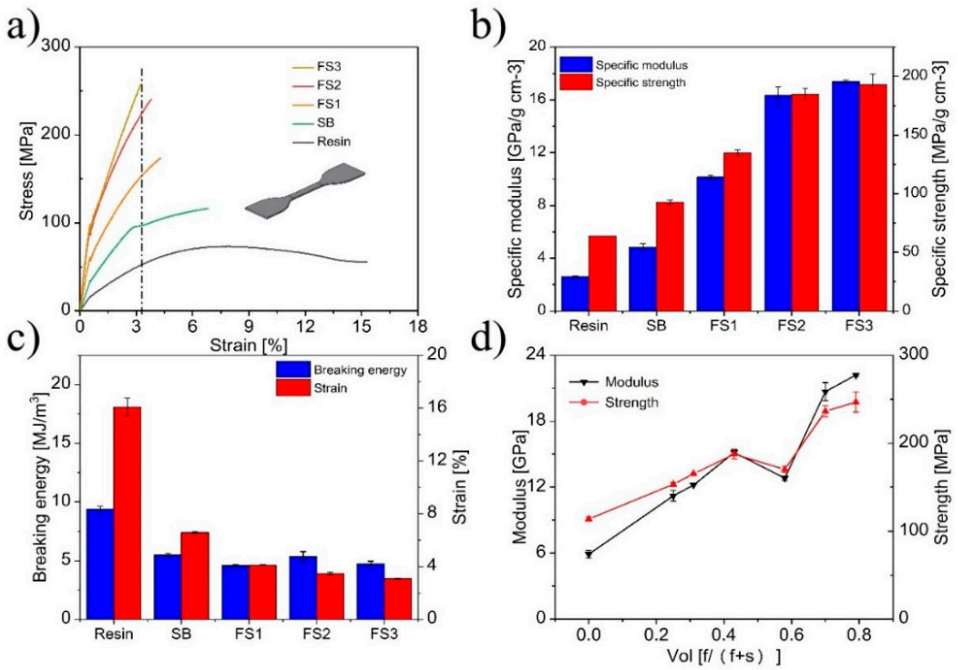

Figure 1. Tensile mechanical properties of the composites studied. (**a**) Stress–strain curve, (**b**) specific Young's modulus and specific strength, (**c**) breaking energy and (**d**) modulus and strength vs. volume fraction. This figure was obtained under kind permission from [37].

For the FS family, it is clear that the Young's modulus increases by incorporating flax fiber. For the symmetric super-hybrid composites (as originally named), the values were compared to the ones obtained with a 42:59 silk/flax ratio and with the flax-reinforced composite. It is clear that the Young's modulus is directly dependent on the flax fiber ratio. The SHS and SHI composites presented similar values compared to the FF composite. Reis et al. [48] proposes a schematic representation of the stress transferring of PEI composites and epoxy resin. In this case, and when analogically comparing with our study, when the reinforcement is equally distributed to the system, the stress transfer tends to be equally distributed. It is noteworthy to mention that the stress transferring can considerably differ depending on the reinforcement arrangement.

Table 2. Tensile mechanical properties for the epoxy resin and the composite studied.

Composite	Young's Modulus (GPa)	Tensile Strength (MPa)	Tensile Breaking Strain (%)
Silk-reinforced/SB	5.90 ± 0.4	113.7 ± 2.4	6.6 ± 0.1
Silk/flax hybrid fiber-reinforced-FS1	12.8 ± 0.2	170.2 ± 3.5	4.1 ± 0.0
Silk/flax hybrid fiber-reinforced-FS2	20.7 ± 0.8	236.4 ± 6.3	3.5 ± 0.1
Silk/flax hybrid fiber-reinforced-FS3	22.2 ± 0.2	246.7 ± 11	3.1 ± 0.0
Silk/flax hybrid fiber-reinforced-HSH	15.2 ± 0.2	187.6 ± 5.5	3.2 ± 0.0
Silk/flax hybrid fiber-reinforced-SHS	11.2 ± 0.5	153.2 ± 2.1	3.3 ± 0.0
Silk/flax hybrid fiber-reinforced-SHI	12.2 ± 0.0	165.3 ± 0.9	3.8 ± 0.0
Flax-reinforced/FF	11.8 ± 0.1	153.2 ± 0.1	3.8 ± 0.0
Pristine epoxy resin	3.00 ± 0.1	73.40 ± 0.2	16.1 ± 0.7

The tensile strength of typical commercial silkworm silk from *Bombyx mori* is about 0.5 GPa [40] while flax fibers ranges from 1500 to 1800 MPa [49]. Of course, these values are not enough to ensure an improvement in the tensile strength since many variables need to be taken into account such as wettability, adhesion and fiber/matrix stress transferring, for example. The tensile strength followed the same trend in the Young's modulus while the breaking strain increased, i.e., a higher rigidity lowers the elongation of the material.

Scheme 4 shows a schematic representation of the stress transferring of two distinct composites: alternatively disposed layers and an in-block composite. This schematic representation is also found in a mathematical simulation for composites [50,51]. In the case of SHI, as alternative layers of stronger and weaker interfacial bonding are found, the overall resistance also decreases. In the beginning, the resistance can be high due to the high resistance of the silk/flax layer, but there is an acceleration of the stress transferring (represented by the red line) as the energy passes through the less resistant layers. In the case of a more homogeneous system, the stress transferring is also more similar.

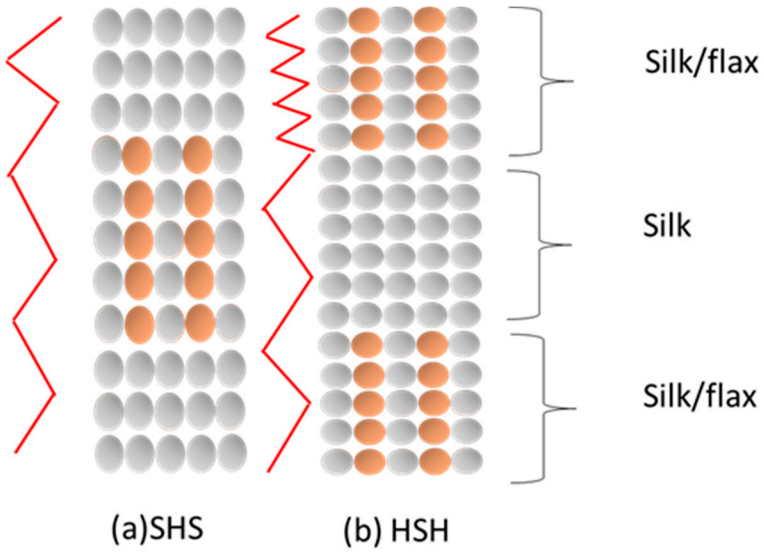

Scheme 4. Schematic representation of the stress transferring of (**a**) alternatively disposed layers and (**b**) in-block layers composite. In the cases above, a rapid stress transfer is visualized in both cases at a specific time, leading to similar Young's modulus values. In the case of FS family, the stress transfer is similar to the upper section of figure (**b**) in all composites, increasing the capacity to store energy and increasing the modulus. The red lines represent the stress transferring speed. The grey circles represent silk fibers while the orange circles represent the flax fibers.

The DMTA curves are showed in Figure 2a–d. The storage modulus (E′) depicted in Figure 2a shows that all curves behave similarly, i.e., a glassy plateau that extends up to a temperature of around 80 °C followed by an abrupt decay until it reaches the elastomeric

state. It is also observed that the higher the storage modulus temperature, the higher the loss of the storage modulus as the material passes through the glass-transition region. A lower E′ was obtained for the neat resin. The curves for SB and SHS were similar, while for the intraply composites a higher modulus was obtained, following the same behavior presented for the flexural modulus. The interplay composite HSH (similar silk and flax volume fraction) presented a similar E′ to FS2 composites. For neat polymers, the storage modulus is attributed to the intermolecular forces and the way that the polymeric chains are packed, while for composite materials, it is attributed to several factors such as the polymer/fiber interface, fiber-volume fraction, the arrangement of the composite and the orientation of the fiber. It is noteworthy to mention that the storage modulus is due to the response of the polymer and how the molecular chains are affected by the external stress. If more stress is required to impose the deformation in the polymeric chains, the higher the storage modulus result will be. The restriction imposed in the polymeric chains can be due to a better fiber/matrix interface, a higher volume fraction (the fibers have higher elastic modulus than the polymeric matrix), the type of composite arrangement or a combination of them. In other words, there is not a unique effect that can affect the storage modulus for composite materials. Figure 2b shows the tan δ curves for the composites studied. The dissipation energy is higher in the glass-transition region compared to other regions. In the glassy state, the elastic behavior is predominant, while in the elastomeric state, the viscous behavior is predominant. At T_g, there is no specific predominance of any behavior. Phenomenologically, in the glassy state, the external stress received as energy is received and absorbed by the polymeric chains. As the energy increases, the movement of the chains becomes more frequent, and the polymeric chains break apart from each other due to the increase in the molecular vibration until they reach the glass-transition temperature; here, the energy is absorbed, dissipated as heat and there is an expansion of the volume of the material, decreasing the mechanical properties and increasing the energy dissipation. The interface lowers the energy dissipation, because the interface is able maintain this energy and transfers it to the fibers. Hence, it is expected that higher energy will be dissipated for the neat resin due to the absence of the fiber/polymer interface. Figure 2c shows that the storage modulus ate two distinct temperatures (at glassy and elastomeric states). It should be noted that there is a considerable decrease in the temperature of the properties due to an increase in the internal energy of the systems, which leads to an increase in the molecular motion of the polymeric chains. The E′s at 140 °C are quite similar for all materials studied, showing that the energetic state is very similar for all composites, while in the glassy state, the reinforcement effect is more easily observed. The storage modulus also increases with the volume fraction (Figure 2d) due to higher restrictions imposed on the molecular chain mobility.

The storage modulus curves were used to estimate the reinforcement coefficient (using the E′ curves) and the constrained region (using the tan δ curves). The extraction of the data was obtained using OriginLab 9.0 Program. The coefficient of reinforcement (C_r) (Equation (1)) was estimated, considering that the modulus values do not start at the same starting point. Also, since the reinforcement effect is usually obtained in the elastomeric state [46], the C_r parameter standardizes the curves and helps to visualize the behavior of the curves. It is noteworthy to mention that for high-modulus structural composites, the reinforcement effect is observed at the glassy state [46] (in this case, so much energy is stored in the glassy state that a rupture of the specimens occurs when the temperature exceeds the glassy state and considerable molecular motion takes place), but for most natural fiber-reinforced composites, the main difference is observed at the elastomeric state [4]. This is due to the fact that the natural reinforcement is softer than the polymeric matrix and hence no considerable reinforcement effect is observed in the glassy state while in the T_g region; the fibers act as a “non-thermally labile” crystallite, restricting the

molecular movement of the amorphous chains of the epoxy resin. Hence, the decrease in the modulus is smoother from the glassy state to the elastomeric state.

$$C_r = \frac{\left(E_g / E_r\right)_{composite}}{\left(E_g / E_r\right)_{epoxy\ resin}} \times 1000 \quad (1)$$

where E_g is the storage modulus obtained at 40 °C (glassy state) and E_r is the rubbery (elastomeric) modulus obtained at 160 °C. The lower the difference between the modulus of two distinct regions, the lower the C_r value.

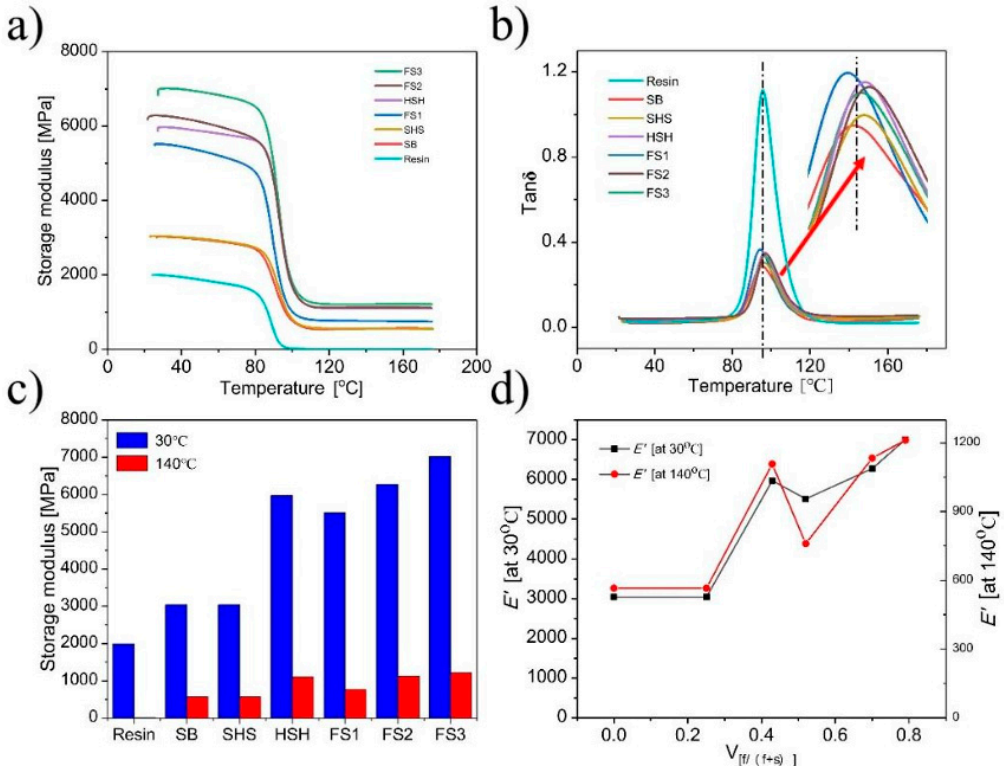

Figure 2. Dynamic mechanical thermal analysis of the composites studied: (**a**) storage moduli curves, (**b**) tan δ curves, (**c**) storage modulus compared at two distinct temperatures (glassy and elastomeric states) and (**d**) storage modulus values at two distinct temperatures plotted against the fiber-volume fraction. This figure was obtained under kind permission from [37].

When the sample passes from the glassy to the elastomeric region, the energy dissipation occurs faster in a short time interval. If the polymer/matrix interface is strong, the maximum peak height is reduced because the interface retains a great portion of energy. If the interface is weaker, a higher dissipation maximum is observed because the stress transferring is not effective and a huge portion of the energy is not retained at the interface. This can be quantified using the constrained region (C), as demonstrated in Equation (2) [46]:

$$C = 1 - \frac{(1 - C_0) \times W}{W_0} \quad (2)$$

where C_0 and W_0 are the volume fraction of the constrained region and the energy loss fraction of the epoxy resin, respectively. C_0 is assumed to be zero for epoxy, while W_0 is the $tan\delta$ area of the epoxy. W is the energy loss fraction of the composite at the $tan\delta$ peak maximum given by $W = (\pi tan\delta\ /\ \pi tan\delta + 1)$, i.e., the area under the curve. Table 3 presents the results of the glass-transition temperature and the constrained region obtained from the $tan\delta$ curves.

Table 3. Glass-transition temperature and constrained region for the studied composites.

Composite	Reinforcement Coefficient	T_g (°C)	Constrained Region
Silk-reinforced/SB	2.50	94 *	0.74
Silk/flax hybrid fiber-reinforced-FS1	3.44	94 *	0.65
Silk/flax hybrid fiber-reinforced-FS2	2.54	97	0.67
Silk/flax hybrid fiber-reinforced-FS3	2.69	96	0.69
Silk/flax hybrid fiber-reinforced-HSH	2.31	96	0.67
Silk/flax hybrid fiber-reinforced-SHS	2.50	96	0.72
Silk/flax hybrid fiber-reinforced-SHI	-	-	-
Flax-reinforced/FF	-	-	-
Epoxy resin	-	95 *	-

* Data obtained from the original study. The other T_g values were obtained using the OriginLab 9.0 Program.

The reinforcement coefficient is lower for the HSH composite and higher for the FS1 composite. Lower values indicate a lower difference between the glassy and the elastomeric states at 40 °C and 160 °C, which is indicative of a higher coefficient of reinforcement. This parameter is independent of the initial values of the storage modulus, i.e., a higher modulus at the glassy state did not reflect a higher or lower C_r. In other words, C_r indicates the capacity of the composite in maintaining the reinforcement effect as the molecular motion of the polymeric chains considerably increases when the temperature passes from the glassy to the elastomeric region.

Regarding Table 2, it is noted that the glass-transition values differ from each other by ~3 °C, which can be considered quite constant. The constrained region is higher for the SB and SHS (0.74 and 0.72, respectively) composites when compared to others. The constrained region is lower for the FS1 (0.65) composite. Higher values are indicative of the immobilized regions' increase and a decrease in the overall molecular mobility. It is also important to mention that there is not a trend among the composites regarding the storage modulus values at the glassy state, the glass-transition temperature and the constrained region, i.e., a higher E′ is not indicative of a higher T_g and a higher constrained region. It should be noted that the higher the storage modulus at the glassy state, the higher the dissipation energy at T_g (due to the higher the energy stored) and hence the lower the constrained region. In other words, the constrained region is directly dependent on the thermal mechanical history of the composite. Phenomenologically, a higher E′ in the glassy state means that a higher amount of energy is required to deform the amorphous polymeric chains, promoted by the type of arrangement that causes a more effective stress transfer though the composite interface. It is noteworthy to mention that the E′ response is from the polymeric matrix and that variations are attributed to how the fiber arrangements and/or polymer/fiber interface interferes in the polymer chain mobility. In general, a higher modulus in the glassy state means that more energy is stored in this region, and as the temperature increases and passes though the glass transition, more energy is dissipated as heat. If the energy dissipation occurs in a short time interval, the modulus loss is usually higher, occasionally leading to a rupture of the composite. In cases where the energy dissipation occurs in a wider temperature range, it can be assumed that the material does not present a fragile behavior but a ductile behavior instead. In these cases, the number of differences between the modulus in the glassy and elastomeric states is lower.

4. Conclusions

This study focused on hybrid silk/flax composites, exploring their quasi-static mechanical properties and dynamic mechanical thermal properties (DMTA). The search for the combination of eco-friendly products with satisfactory mechanical properties has driven researchers to explore innovative combinations of materials. In this investigation, silk and flax fibers were artfully combined in various configurations, yielding eight distinct

composites. The focus was on understanding the intricate relationship between structure and properties, while building upon the existing work of Liu et al. [38].

The primary findings of this study shed light on the remarkable synergistic effects achieved through the strategic arrangements of flax and silk fibers. This combination resulted in the creation of tailor-made composites that offered both cost-efficiency and high-performance characteristics. These insights promise to play a crucial role in advancing the field of natural fiber composites, particularly in the context of hybrid materials and their applications.

The mechanical properties revealed a range of behaviors among the composites, with flax-reinforced variants exhibiting higher Young's moduli than pure silk-reinforced composites. These variations were attributed to different composite configurations and the quality of matrix/fiber interfaces. The manner in which stress is transferred between the amorphous polymeric chains and fibers at these interfaces played a significant role in determining the overall mechanical properties. These findings underscored the critical role of interface quality and fiber resistance governing composite behavior.

Dynamic mechanical thermal analysis further elucidated the properties of these hybrid composites. Parameters such as the reinforcement coefficient (C_r) and constrained region were examined. The C_r highlighted the capacity of composites to maintain their reinforcement effect as molecular motion within the polymeric matrix increased. Meanwhile, the constrained region offered insights into the immobilized regions and molecular mobility within the composite.

Overall, this study represents a valuable contribution to the field of natural fiber composites. It not only corroborated and expanded upon existing research but also offered fresh perspectives on the structure–property relationship in these hybrid materials. These insights have the potential to drive innovation in the development of eco-friendly and high-performance composite materials for various applications, ranging from automotive components to biomedical devices. As the world continues to prioritize sustainability, the pursuit of such hybrid materials holds great promise for the future of materials science and engineering.

Author Contributions: Conceptualization, H.L.O.J.; methodology, H.L.O.J.; validation, H.L.O.J., R.M.N. and E.K.; formal analysis, L.K.L. and L.D.A.; investigation, H.L.O.J.; writing—original draft preparation, H.L.O.J. and L.D.A.; writing—review and editing, R.M.N., E.K. and L.K.L.; visualization, E.K.; supervision, H.L.O.J.; project administration, H.L.O.J. All authors have read and agreed to the published version of the manuscript.

Funding: This research received no external funding.

Data Availability Statement: Data are contained within the article.

Conflicts of Interest: The authors declare no conflicts of interest.

References

1. Satyanarayana, K.G.; Arizaga, G.G.C.; Wypych, F. Biodegradable composites based on lignocellulosic fibers-An overview. *Prog. Polym. Sci.* **2009**, *34*, 982–1021. [CrossRef]
2. Kandasamy, J.; Soundhar, A.; Rajesh, M.; Mallikarjuna Reddy, D.; Kar, V.R. Natural Fiber Composite for Structural Applications. In *Structural Health Monitoring System for Synthetic, Hybrid and Natural Fiber Composites*; Springer: Singapore, 2021; pp. 23–35.
3. Ornaghi, H.L.; Monticeli, F.M.; Neves, R.M.; Zattera, A.J.; Cioffi, M.O.H.; Voorwald, H.J.C. Effect of stacking sequence and porosity on creep behavior of glass/epoxy and carbon/epoxy hybrid laminate composites. *Compos. Commun.* **2020**, *19*, 210–219. [CrossRef]
4. Angrizani, C.C.; Ornaghi, H.L.; Zattera, A.J.; Amico, S.C. Thermal and Mechanical Investigation of Interlaminate Glass/Curaua Hybrid Polymer Composites. *J. Nat. Fibers* **2017**, *14*, 271–277. [CrossRef]
5. Ornaghi, H.L.; Ornaghi, F.G.; de Carvalho Benini, K.C.C.; Bianchi, O. A comprehensive kinetic simulation of different types of plant fibers: Autocatalytic degradation mechanism. *Cellulose* **2019**, *26*, 7145–7157. [CrossRef]
6. Thyavihalli Girijappa, Y.G.; Mavinkere Rangappa, S.; Parameswaranpillai, J.; Siengchin, S. Natural Fibers as Sustainable and Renewable Resource for Development of Eco-Friendly Composites: A Comprehensive Review. *Front. Mater.* **2019**, *6*, 226. [CrossRef]

7. Asim, M.; Paridah, M.T.; Chandrasekar, M.; Shahroze, R.M.; Jawaid, M.; Nasir, M.; Siakeng, R. Thermal stability of natural fibers and their polymer composites. *Iran. Polym. J.* **2020**, *29*, 625–648. [CrossRef]
8. Chokshi, S.; Parmar, V.; Gohil, P.; Chaudhary, V. Chemical Composition and Mechanical Properties of Natural Fibers. *J. Nat. Fibers* **2022**, *19*, 3942–3953. [CrossRef]
9. Ornaghi Jr, H.L.; Faccio, M.; Soares, M.R.F. Thermal degradation kinetics of natural fibers: Determination of the kinetic triplet and lifetime prediction. *Polyssacharides* **2024**, *27*, 169–183. [CrossRef]
10. Neto, J.; Queiroz, H.; Aguiar, R.; Lima, R.; Cavalcanti, D.; Banea, M.D. A review of recent advances in hybrid natural fiber reinforced polymer composites. *J. Renew. Mater.* **2022**, *10*, 561–589. [CrossRef]
11. Arslanoglu, F.; AytaÇ, S. The Important in Terms of Health of Flax (*Linum usitatissimum* L.). *Int. J. Life Sci. Biotechnol.* **2020**, *3*, 95–107. [CrossRef]
12. More, A.P. Flax fiber–based polymer composites: A review. *Adv. Compos. Hybrid Mater.* **2022**, *5*, 1–20. [CrossRef]
13. Moudood, A.; Rahman, A.; Öchsner, A.; Islam, M.; Francucci, G. Flax fiber and its composites: An overview of water and moisture absorption impact on their performance. *J. Reinf. Plast. Compos.* **2019**, *38*, 323–339. [CrossRef]
14. Prashanth, M.; Gouda, P.S.S.; Manjunatha, T.S.; Banapurmath, N.R.; Edacheriane, A. Understanding the impact of fiber orientation on mechanical, interlaminar shear strength, and fracture properties of jute–banana hybrid composite laminates. *Polym. Compos.* **2021**, *42*, 5475–5489. [CrossRef]
15. Mahesh, V.; Joladarashi, S.; Kulkarni, S.M. An experimental study on adhesion, flexibility, interlaminar shear strength, and damage mechanism of jute/rubber-based flexible "green" composite. *J. Thermoplast. Compos. Mater.* **2022**, *35*, 149–176. [CrossRef]
16. Nightingale, C.; Day, R.J. Flexural and interlaminar shear strength properties of carbon fiber/epoxy composites cured thermally and with microwave radiation. *Compos.-Part A Appl. Sci. Manuf.* **2002**, *33*, 1021–1030.
17. Jarukumjorn, K.; Suppakarn, N. Effect of glass fiber hybridization on properties of sisal fiber-polypropylene composites. *Compos. Part. B Eng.* **2009**, *40*, 623–627. [CrossRef]
18. Monjon, A.; Santos, P.; Valvez, S.; Reis, P.N.B. Hybridization Effects on Bending and Interlaminar Shear Strength of Composite Laminates. *Materials* **2022**, *15*, 1302. [CrossRef]
19. Sanjay, M.R.; Arpitha, G.R.; Senthamaraikannan, P.; Kathiresan, M.; Saibalaji, M.A.; Yogesha, B. The Hybrid Effect of Jute/Kenaf/E-Glass Woven Fabric Epoxy Composites for Medium Load Applications: Impact, Inter-Laminar Strength, and Failure Surface Characterization. *J. Nat. Fibers* **2019**, *16*, 600–612.
20. Saidane, E.H.; Scida, D.; Pac, M.J.; Ayad, R. Mode-I interlaminar fracture toughness of flax, glass and hybrid flax-glass fiber woven composites: Failure mechanism evaluation using acoustic emission analysis. *Polym. Test* **2019**, *75*, 246–253. [CrossRef]
21. Ranakoti, L.; Gupta, M.K.; Rakesh, P.K. Silk and Silk-Based Composites: Opportunities and Challenges. In *Processing of Green Composites*; Springer: Sinapore, 2019; pp. 91–106.
22. Wu, C.; Egawa, S.; Kanno, T.; Kurita, H.; Wang, Z.; Iida, E.; Narita, F. Nanocellulose reinforced silkworm silk fibers for application to biodegradable polymers. *Mater. Des.* **2021**, *202*, 109537. [CrossRef]
23. Yang, K.; Wu, Z.; Zhou, C.; Cai, S.; Wu, Z.; Tian, W.; Wu, S.; Ritchie, R.O.; Guan, J. Comparison of toughening mechanisms in natural silk-reinforced composites with three epoxy resin matrices. *Compos. Part A Appl. Sci. Manuf.* **2022**, *154*, 106760. [CrossRef]
24. Guo, C.; Zhang, J.; Jordan, J.S.; Wang, X.; Henning, R.W.; Yarger, J.L. Structural Comparison of Various Silkworm Silks: An Insight into the Structure-Property Relationship. *Biomacromolecules* **2018**, *19*, 906–917. [CrossRef] [PubMed]
25. Yang, K.; Ritchie, R.O.; Gu, Y.; Wu, S.J.; Guan, J. High volume-fraction silk fabric reinforcements can improve the key mechanical properties of epoxy resin composites. *Mater. Des.* **2016**, *108*, 470–478. [CrossRef]
26. Das, S.; Natarajan, G. Chapter 10—Silk fiber composites in biomedical applications. In *Materials for Biomedical Engineering*; Elsevier: Amsterdam, The Netherlands, 2019; pp. 309–338.
27. Hardy, J.G.; Scheibel, T.R. Composite materials based on silk proteins. *Prog. Polym. Sci.* **2010**, *35*, 1093–1115. [CrossRef]
28. Li, Y.; Hu, C.; Yu, Y. Interfacial studies of sisal fiber reinforced high density polyethylene (HDPE) composites. *Compos. Part A Appl. Sci. Manuf.* **2008**, *39*, 570–578. [CrossRef]
29. Bera, M.; Alagirusamy, R.; Das, A. A study on interfacial properties of jute-PP composites. *J. Reinf. Plast. Compos.* **2010**, *29*, 3155–3161. [CrossRef]
30. Araujo, J.R.; Mano, B.; Teixeira, G.M.; Spinacé, M.A.S.; De Paoli, M.A. Biomicrofibrilar composites of high density polyethylene reinforced with curauá fibers: Mechanical, interfacial and morphological properties. *Compos. Sci. Technol.* **2010**, *70*, 1637–1644. [CrossRef]
31. Karthi, N.; Kumaresan, K.; Sathish, S.; Gokulkumar, S.; Prabhu, L.; Vigneshkumar, N. An overview: Natural fiber reinforced hybrid composites, chemical treatments and application areas. *Mater. Today Proc.* **2019**, *27*, 2828–2834. [CrossRef]
32. Neves, R.M.; Monticelli, F.M.; Almeida Jr, H.; Ornaghi Jr, H. Hybrid Vegetable/Glass Fiber Epoxy Composites: A Systematic Review. In *Vegetable Fiber Composites and Their Technological Applications*; Springer: Berlin/Heidelberg, Germany, 2021; p. 6.
33. Saleem, A.; Medina, L.; Skrifvars, M.; Berglin, L. Hybrid Polymer Composites of Bio-Based Bast Fibers with Glass, Carbon and Basalt Fibers for Automotive Applications—A Review. *Molecules* **2020**, *25*, 4933. [CrossRef]
34. Safri, S.N.A.; Sultan, M.T.H.; Jawaid, M.; Jayakrishna, K. Impact behaviour of hybrid composites for structural applications: A review. *Compos. Part B Eng.* **2018**, *133*, 112–121. [CrossRef]
35. Darshan, S.M.; Suresha, B. Effect of basalt fiber hybridization on mechanical properties of silk fiber reinforced epoxy composites. *Mater. Today Proc.* **2020**, *43*, 986–994. [CrossRef]

36. Huang, X.; Zhang, M.; Ming, J.; Ning, X.; Bai, S. High-Strength and High-Toughness Silk Fibroin Hydrogels: A Strategy Using Dynamic Host-Guest Interactions. *ACS Appl. Bio. Mater.* **2020**, *3*, 7103–7112. [CrossRef] [PubMed]
37. Wu, C.; Yang, K.; Gu, Y.; Xu, J.; Ritchie, R.O.; Guan, J. Mechanical properties and impact performance of silk-epoxy resin composites modulated by flax fibers. *Compos. Part A Appl. Sci. Manuf.* **2019**, *117*, 357–368. [CrossRef]
38. Liu, X.; Zhang, K.-Q. Silk Fiber—Molecular Formation Mechanism, Structure- Property Relationship and Advanced Applications. *Oligomerization Chem. Biol. Compd.* **2014**, *3*, 57611.
39. Yang, K.; Gu, Y.; Xu, J.; Ritchie, R.O.; Guan, J. Data for: Mechanical properties and impact performance of silk-epoxy resin composites modulated by flax fibers. *Mendeley Data* **2018**, *V1*, 17632.
40. Baley, C. Analysis of the flax fibers tensile behaviour and analysis of the tensile stiffness. *Compos. Part A* **2002**, *33*, 939–948. [CrossRef]
41. Menard, K.P.; Menard, N.R. *Dynamic Mechanical Analysis*; CRC Press: Boca Raton, FL, USA, 1990; Volume 31.
42. Khandelwal, S.; Rhee, K.Y. Recent advances in basalt-fiber-reinforced composites: Tailoring the fiber-matrix interface. *Compos. Part B Eng.* **2020**, *192*, 108011. [CrossRef]
43. Zhang, B.; Jia, L.; Tian, M.; Ning, N.; Zhang, L.; Wang, W. Surface and interface modification of aramid fiber and its reinforcement for polymer composites: A review. *Eur. Polym. J.* **2021**, *147*, 110352. [CrossRef]
44. Ferry, J.D.; Myers, H.S. *Viscoelastic Properties of Polymers*; John Wiley & Sons, Inc.: Hoboken, NJ, USA, 1961; Volume 108.
45. Poletto, M.; Ornaghi Júnior, H.L.; Visakh, P.M.; Arao, Y. Composites and Nanocomposites Based on Renewable and Sustainable Materials. *Int. J. Polym. Sci.* **2016**, *2016*, 2–4. [CrossRef]
46. Ornaghi Júnior, H.L.; Zattera, A.J.; Amico, S.C. Dynamic Mechanical Properties and Correlation With Dynamic Fragility of Sisal Reinforced Composites. *Polym. Compos.* **2015**, *36*, 161–166. [CrossRef]
47. Tham, M.W.; Fazita, M.N.; Abdul Khalil, H.P.S.; Mahmud Zuhudi, N.Z.; Jaafar, M.; Rizal, S.; Haafiz, M.M. Tensile properties prediction of natural fiber composites using rule of mixtures: A review. *J. Reinf. Plast. Compos.* **2019**, *38*, 211–248. [CrossRef]
48. dos Reis, A.K.; Monticelli, F.M.; Neves, R.M.; de Paula Santos, L.F.; Botelho, E.C.; Luiz Ornaghi, H. Creep behavior of polyetherimide semipreg and epoxy prepreg composites: Structure vs. property relationship. *J. Compos. Mater.* **2020**, *54*, 4121–4131. [CrossRef]
49. Bosh, L.; Vandenoever MJ, A.; Petersat OC, J. Tensile and compressive properties of flax fibres.1023_A-1014925621252. *J. Mater. Sci.* **2002**, *37*, 1683–1692. [CrossRef]
50. Xia, Z.; Okabe, T.; Curtin, W.A. Shear-lag versus finite element models for stress transfer in fiber-reinforced composites. *Compos. Sci. Technol.* **2002**, *62*, 1141–1149. [CrossRef]
51. Swolfs, Y.; Verpoest, I.; Gorbatikh, L. Maximising the hybrid effect in unidirectional hybrid composites. *Mater. Des.* **2016**, *93*, 39–45. [CrossRef]